

# Impact of early stage non-equilibrium dynamics on photon production in relativistic heavy ion collisions

L Oliva<sup>1,2</sup>, M Ruggieri<sup>3</sup>, S Plumari<sup>1,2</sup>, F Scardina<sup>1,2</sup> and V Greco<sup>1,2</sup>

<sup>1</sup> Department of Physics and Astronomy, University of Catania, Via S. Sofia 64, 95123 Catania, Italy

<sup>2</sup> INFN-Laboratori Nazionali del Sud, Via S. Sofia 62, 95123 Catania, Italy

<sup>3</sup> College of Physics, University of Chinese Academy of Sciences, Yuquanlu 19A, Beijing 100049, China

E-mail: [lucia.oliva@lns.infn.it](mailto:lucia.oliva@lns.infn.it)

**Abstract.** In this study we discuss our results on the spectrum of photons emitted from the quark-gluon plasma produced in heavy ion collisions at RHIC energies. Simulating the space-time evolution of the fireball by solving the relativistic Boltzmann transport equation and including two-particle scattering processes with photon emission allows us to make a first step in the description of thermal photons from the QGP as well as of those produced in the pre-equilibrium stage. Indeed, we consider not only a standard Glauber initial condition but also a model in which quarks and gluons are produced in the very early stage through the Schwinger mechanism by the decay of an initial color-electric field. In the latter approach relativistic kinetic equations are coupled in a self-consistent way to field equations. We aim at spotting the impact of early stage non-equilibrium dynamics on the photon production.

## 1. Introduction

Radiation of photons is considered an important and efficient probe to scrutinise the properties of the quark-gluon plasma. While hadrons are emitted from the freeze-out surface after suffering intense scatterings, photons are radiated during the whole spacetime history of the expanding fireball and, due to their electromagnetic nature, leave the system almost undisturbed, reaching the detector with the unaltered imprint of the circumstances of their production, which takes place from the initial stage up to the final one.

In heavy ion collisions, besides photons coming from hadron decay, there are photons emerging directly from collision processes, called *direct photons*, whose main categories are: *prompt* photons, which originate from initial hard scatterings; *pre-equilibrium* photons, produced before medium thermalization; *thermal* photons from qgp as well as from hadron gas. While thermal and prompt photons are quite well described, a good knowledge of photon emission in the initial out-of-equilibrium stage of heavy ion collision is still missing. Then, it is of particular interest to compute photon production in the initial stage of the system produced by the collision.

In the standard picture that describes the high energy nuclear collisions, after the two incoming nuclei had passed one through each other, a particular configuration of longitudinal color-electric and color-magnetic fields, named *Glasma*, is produced.

We model early time dynamics of relativistic heavy ion collisions assuming a longitudinal color-electric field which decays to gluon and quark-antiquark pairs through the Schwinger



effect; we couple in a self-consistent way the evolution equation of the initial field to the relativistic transport equation, which describes the evolution of the many-particle system and how it achieves an isotropic and thermalized state by means of collisions. In this talk we present our recent results about photon emission from the quark-gluon plasma, investigating the effect of pre-equilibrium dynamics on photon spectrum.

## 2. Modelling pre-equilibrium dynamics of relativistic heavy ion collisions

In this section we briefly explain how we simulate in our model the early stages of ultra-relativistic heavy ion collision; see Ref. [1] for further details.

### 2.1. Abelian flux tube model and Schwinger mechanism

We implement the Abelian Flux Tube (AFT) model [1, 2] with an initial condition constituted by a purely longitudinal color-electric field, neglecting for simplicity color-magnetic fields which should be considered in a more appropriate description of the Glasma state. We also assume the initial field is boost-invariant along the longitudinal direction and we ignore initial transverse fields that are produced by quantum fluctuations. The initial field then decays into particle quanta by the Schwinger mechanism, which predicts pair formation in a strong electric field [3].

In a static box the decay probability of a color-electric field  $E$  in massless particles is

$$\frac{dN_{jc}}{d\Gamma} \equiv p_0 \frac{dN_{jc}}{d^4x d^2p_T dp_z} = \frac{\mathcal{E}_{jc}}{4\pi^3} \left| \ln \left( 1 \pm e^{-\pi p_T^2 / \mathcal{E}_{jc}} \right) \right| \delta(p_z) p_0, \quad (1)$$

where the plus (minus) sign corresponds to the creation of a boson (fermion-antifermion) pair, the momentum components  $p_T$  and  $p_z$  refer to each of the two particles created from the vacuum and  $p_0 = \sqrt{p_T^2 + p_z^2}$  is the single particle kinetic energy.  $\mathcal{E}$  is the effective force acting on the tunnelling pair and depending on color and flavor; it is given by  $\mathcal{E}_{jc} = (g|Q_{jc}E| - \sigma_j) \theta(g|Q_{jc}E| - \sigma_j)$ , where  $\sigma_j$  corresponds to the string tension depending on the flavor considered. The  $Q_{jc}$  are color-flavor charges which in the case of quarks are  $Q_{j1} = 1/2$ ,  $Q_{j2} = -1/2$ ,  $Q_{j3} = 0$ , for  $j = 1, N_f$ ; for antiquarks, corresponding to negative values of  $j$ , the color-flavor charges are just minus the corresponding charges for quarks; finally for gluons (labelled with  $j = 0$ ) the charges are  $Q_{01} = 1$ ,  $Q_{02} = 1/2$ ,  $Q_{03} = -1/2$ ,  $Q_{04} = -Q_{01}$ ,  $Q_{05} = -Q_{02}$ ,  $Q_{06} = -Q_{03}$ . We have only six gluons corresponding to the non-diagonal color generators, because we assume that the initial color field is polarized along the third direction of adjoint color space; the two gluon fields corresponding to the diagonal color generators do not couple with the background field, hence they cannot be produced by the Schwinger mechanism. Eq. 1 is then easily generalized to the case of an expanding box, see [1, 2].

### Relativistic transport theory and field equations

The dynamics of the many-particle system produced by the decay of the color-electric field is described by the relativistic Boltzmann transport equation:

$$\left( p^\mu \partial_\mu + g Q_{jc} F^{\mu\nu} p_\nu \partial_\mu^p \right) f_{jc}(x, p) = \frac{dN_{jc}}{d\Gamma} + C_{jc}[f], \quad (2)$$

where  $f_{jc}(x, p)$  is the distribution function for flavor  $j$  and color  $c$  and  $F^{\mu\nu}$  is the color-electromagnetic tensor. On the right hand side  $dN/d\Gamma$  is the invariant source term, which accounts for creation of pairs given by Eq. 1, and  $C[f]$  represents the collision integral, which describes how  $f$  changes due to collision processes and is responsible for a finite value of the viscosity. We solve numerically the Boltzmann equation on a tridimensional lattice and using the test particle method to sample  $f(x, p)$ ; the collision integral is computed by means of a stochastic algorithm [4, 5, 6, 7, 8, 9, 10]. With this theoretical approach one can follow the

entire dynamical evolution of the system produced in relativistic heavy ion collisions. Although usual inputs of a transport code are cross sections of a fixed set of microscopic processes, in our model we start from a fixed viscosity over entropy density ratio  $\eta/s \neq 0$  and compute cross sections according to the Chapman-Enskog equation [8].

Assuming an Abelian dynamics, the evolution equations for the color-electric field are the Maxwell equations:

$$\nabla \cdot \mathbf{E} = \rho, \quad \frac{\partial \mathbf{E}}{\partial t} = -\mathbf{J}, \quad (3)$$

where  $t$  is the time in the laboratory frame. The initial field is only longitudinal, whereas transverse components of  $\mathbf{E}$  will be generated by transverse currents according to Eq. 3. The total current is  $\mathbf{J} = \mathbf{J}_D + \mathbf{J}_M$ , where the *displacement current*  $\mathbf{J}_D$  is due to the dipoles created by the Schwinger effect and the *matter current*  $\mathbf{J}_M$  depends on the motion of the charges. Since color charges and currents depend on parton distribution functions as well as the kinetic equations, we solve field and particles equations self-consistently, taking into account the back-reaction of particles on the field. We notice that, even if the equation of motion of the classical field is abelian, there is a sign of the non-abelian nature of QCD because the background field interacts with gluon quanta via  $\mathbf{J}_D$ .

### 3. Effect of pre-equilibrium on photon spectrum

In order to simulate photon production we add to the collision integral of Eq. 2 the processes with a photon in the final state. In this talk we focus on the  $2 \rightarrow 2$  scatterings, i.e. the QCD Compton scattering  $q/\bar{q} + g \rightarrow q/\bar{q} + \gamma$  and the quark-antiquark annihilation  $q + \bar{q} \rightarrow g + \gamma$ , leaving the inclusion of  $2 \rightarrow 3$  processes and of the LPM effect [11] to future works.

We are interested in grasping the effect of pre-equilibrium stage on direct photon spectrum. For this purpose we compare simulations starting at  $t_0 = 0.01 \text{ fm}/c$  with the model described in the previous section to simulations with an equilibrium initial condition. The latter is based on the Glauber model, with an  $x$ -space distribution given by the a standard mixture  $0.85N_{part} + 0.15N_{coll}$  and a  $p$ -space thermalized spectrum in the transverse plane at a time  $t_0 = 0.6 \text{ fm}/c$  with a maximum initial temperature  $T_0 = 340 \text{ MeV}$ . Following Ref. [9] we call this case *Th-Glauber*, while we refer to simulations with the Abelian flux tube model as *AFT-Schwinger*. In this study we focus on RHIC collision at an impact parameter  $b = 7.5 \text{ fm}$ .

In the AFT-Schwinger simulation we assume the initial chromo-electric field is boost invariant in the longitudinal direction and smooth in transverse plane, with the specific configuration given by a Glauber-type distribution:

$$E_z^0(x, y) = E_{max}^0 (c_c \rho_{coll}(x, y) + c_p \rho_{part}(x, y)), \quad (4)$$

with  $c_p = 1 - c_c$ . The two free parameters  $E_{max}^0$  and  $c_c$  are fixed in order to match at  $t_0 = 0.6 \text{ fm}/c$  particle multiplicity and eccentricity with those of the Th-Glauber case at initial time. For RHIC collision at  $b = 7.5 \text{ fm}$  we obtain an initial longitudinal field with  $E_{max}^0 = 3.3 \text{ GeV}^2$  and  $c_c = 0.6$ .

In Fig. 1 we plot our result for photon spectrum (main panel) and photon number (inset panel) obtained in the Th-Glauber and in the AFT-Schwinger cases. We show also the curve obtained with the AFT-Schwinger model in which photon production is artificially started at  $0.6 \text{ fm}/c$ ; comparing the latter with the Th-Glauber case, we notice that both photon spectrum and photon number are similar in the two simulations, meaning that the system evolves in the same way after  $0.6 \text{ fm}/c$  with Glauber and non-equilibrium initial conditions. Thus, we can consider the differences between AFT-Schwinger and Th-Glauber curves as due to pre-equilibrium photons. We see that pre-equilibrium photons enhance the total photon number of about 30%, giving a significant contribution at higher transverse momentum, in a  $p_T$  region where thermal emission (both from QGP and from hadron gas) becomes less important.

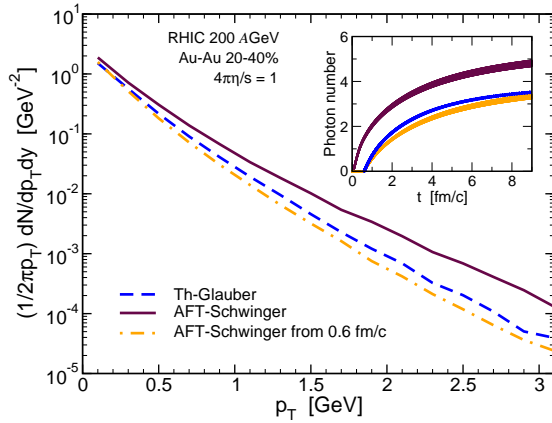


**Figure 1.** Photon spectrum at midrapidity  $|y| < 0.5$  (main panel) and total photon number (inset panel) obtained by AFT-Schwinger (solid maroon line) and Th-Glauber (dashed blue line) simulations. The dot-dashed orange curve corresponds to an AFT-Schwinger simulation in which photon production is enabled from  $t = 0.6$  fm/c.

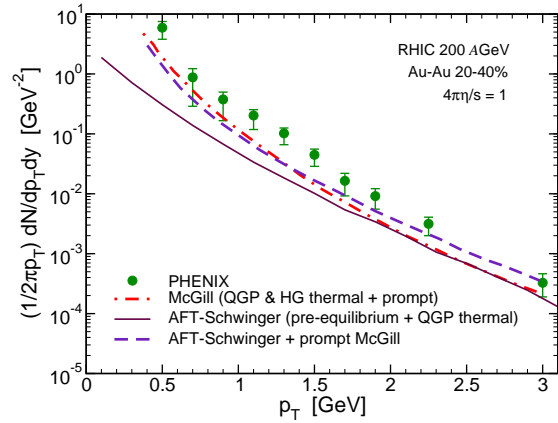


**Figure 2.** Comparison of the final photon spectrum obtained by Paquet et al. from the McGill University [13] (dot-dashed red line) with our results. In the dashed indico curve McGill's prompt photons are added to our AFT-Schwinger result (thin solid maroon line). Experimental data are from PHENIX Collaboration [12].

We stress that we do not compute photon production by integrating photon rate over a spacetime volume, as it is done in hydrodynamics calculations. Indeed, we use scattering matrix elements in the collision integral; this allows to follow photon production since the very early stage as soon as particles pop up from the vacuum.

In Fig. 2 we compare the direct photon spectrum obtained by our AFT-Schwinger simulation with experimental data [12] and with the result of Ref. [13]. The latter includes not only QGP thermal photons but also thermal hadronic emission as well as prompt photons, while does not take into account photon production before QGP equilibration. In the figure we plot also our result in which prompt photons from Ref. [13] are added. We notice that, although we need to include in our simulations higher order photon emission processes as well as hadronic thermal production which would enhance the direct photon yield mainly at  $p_T < 1.5$  GeV, on the other hand our model of the early stages of relativistic heavy ion collision allows to describe pre-equilibrium photons which may reduce the tension between theory and experimental data.

## References

- [1] Ruggieri M, Puglisi A, Oliva L, Plumari S, Scardina F and Greco V 2015 *Phys. Rev. C* **92** 064904
- [2] Ryblewski R and Florkowski W 2013 *Phys. Rev. D* **88** 034028
- [3] Schwinger J S 1951 *Phys. Rev.* **82** 664-79
- [4] Xu Z, Greiner C and Stoecker H 2008 *Phys. Rev. Lett.* **101** 082302
- [5] Xu Z and Greiner C 2009 *Phys. Rev. C* **79** 014904
- [6] Bratkovskaya E L, Cassing W, Konchakovski V P and Linnyk O 2011 *Nucl. Phys. A* **856** 162-82
- [7] Ferini G, Colonna M, Di Toro M and Greco V 2009 *Phys. Lett. B* **670** 325-9
- [8] Plumari S, Puglisi A, Scardina F and Greco V 2012 *Phys. Rev. C* **86** 054902
- [9] Ruggieri M, Scardina F, Plumari S and Greco V 2013 *Phys. Lett. B* **727** 177-81
- [10] Ruggieri M, Scardina F, Plumari S and Greco V 2014 *Phys. Rev. C* **89** 054914
- [11] Arnold P, Moore G D and Yaffe L G 2001 *JHEP* **0112** 009 and references therein
- [12] Adare A et al 2015 *Phys. Rev. C* **91** 064904
- [13] Paquet J F, Shen C, Denicol G S, Luzum M, Schenke B, Jeon S and Gale C 2016 *Phys. Rev. C* **93** 044906